

A Test of Gradient Transport and Its Generalizations

K.R. Sreenivasan

Applied Mechanics, Mason Laboratory, Yale University, New Haven, CT 06520, USA

S. Tavoularis

Mechanical Engineering Department, University of Ottawa, Ontario, Canada K1N 6N5

S. Corrsin

Chemical Engineering Department, Johns Hopkins University, Baltimore, MD 21218, USA

Abstract

Heat flux measurements in several specially designed turbulent flows with inhomogeneous temperature field are presented and analyzed with the purpose of evaluating the performance of the gradient transport models (GTM) as well as several of the generalizations, and of understanding the circumstances in which the GTM works in spite of the a priori conclusions to the contrary. One of the flows considered is a uniform grid-generated flow; two others are shear flows with transverse homogeneity and a constant mean velocity gradient. The fourth is the wake of a circular cylinder in which an asymmetric temperature field is created by heating a combination of thin wires located off-axis. A GTM with a constant turbulent diffusivity adequately describes the turbulent heat flux in all three homogeneous flows, while in the inhomogeneous flow, forcing gradient transport to the measured heat flux results in negative diffusivity over a part of the flow. Direct evaluation from the present and other measurements shows that none of the generalizations of the GTM is adequate. It is suggested that the large eddy transport in inhomogeneous shear flows is the possible cause for the failure of the GTM, and a simple criterion set forth here shows that its apparent success in symmetrically heated free shear flows is largely a happenstance caused by the imposed boundary conditions.

Nomenclature

d	= diameter of the cylinder	u_i	= velocity fluctuation in the direction i
D	= turbulent diffusivity	U_i	= mean velocity in the direction i
h	= height of the wind-tunnel test section	V	= characteristic velocity scale for turbulent diffusion
l_θ	= half the distance between half-maximum θ' points	V_c	= characteristic bulk convection velocity
l	= characteristic length scale for turbulent diffusion, $= V\tau$	w	= wake defect velocity
L_f	= longitudinal integral length scale	x_i	= coordinate axes; $i=1$ is along the flow and $i=2$ is along the (transverse) direction of maximum shear
L_g	= transverse integral length scale	θ	= temperature fluctuation
L_θ	= half the distance between $T_{\max}/2$ points	τ	= characteristic time scale for turbulent diffusion
M	= mesh size of the grid		
q'	$= (\overline{u_i u_i})^{1/2}$		
T	= mean temperature rise above the ambient		

Suffixes

- 0 = centreline value
- max = maximum value
- ' = root-mean-square value

Introduction

Virtually all the “classical turbulent theories” model turbulent transport of momentum, heat or a passive contaminant by linear mean gradient models. This hypothesis, probably attributable to *de St. Venant* or to *Boussinesq*, has appeared in different forms – usually incorporating an ad hoc estimate of the proportionality coefficient, the “eddy viscosity” or “eddy diffusivity” (for example, [1, 2]).

In spite of the enormous development in turbulence modelling witnessed over the last two decades (e.g., [3]), the simplicity of the gradient transport models (GTM) – often with enough adjustable parameters – appears to be responsible for their persistent use in some areas of engineering practice, especially in meteorology and oceanography. The GTM has been used in modelling such diverse physical phenomena as the growth and dispersal of populations [4], the solar radiation in dynamical models of terrestrial climate (for an extensive review, see [5]), etc. It is thus no surprise that a recurring concern has been voiced on the general conditions for the validity of the GTM [6–8]. Among other things, gradient transport models require that the characteristic scale of the turbulent transporting mechanism must be small compared with the dimension characteristic of the inhomogeneity of the mean transported quantity. It has been pointed out several times [6–8] that nearly all turbulent flows violate this basic a priori requirement, and yet a reasonable degree of success has been claimed for the GTMs, especially in free shear flows. Therefore, a study directed towards determining the reasons for this (apparent) success of the GTMs appeared to be worthwhile; this is one of the major goals of the present study.

It is perhaps apt to quote the following from *Saffman* [9] here because it reflects our current concern rather well: “The continual preaching against the eddy diffusivity hypothesis... has not served any useful purpose. The effort would have been better spent trying to understand the reasons for the apparent success and the circumstances in which the hypothesis must (not ought to) fail...”. We hoped that some light would be shed on this issue if measurements were made in the three classes of flows in which a priori arguments would suggest that GTM

- a) ‘ought to’ and does work,
- b) ought not to but does work,
- c) ought not to and does not work.

Clearly, there are no turbulent flows in which GTM ‘ought to’ work, but homogeneous flows offer the best possible chance of success. (We shall briefly return to this point somewhat later.) Consequently, we set up some experiments in homogeneous shear flows. Surprising success has often been claimed for the GTMs in free shear flows, and so we sought to deliberately create conditions in a free shear flow in which GTM would not work. Together, these constituted our experimental effort in this study. Presentation of the experimental data in these flows with a view to spur possible development of more sophisticated turbulence modelling is a secondary purpose of our study.

Several instances can now be quoted which, over the years, have demonstrated the inadequacies of the GTMs [10–19]. Mindful of these inadequacies to turbulence, several formal generalizations have been proposed [8, 20–22]. Alternatively, it has been thought that formal generalizations do not address themselves to the heart of the problem, and so some ad hoc ‘corrections’ (which could even be drastic), based on a totally different physical mechanism, have also been proposed (for example [23]). However, the validity of any of these models in more than one situation remains to be tested. This is the second major purpose of the present study. We tested these various generalizations not only for our flow in which GTM does not work, but also in another similar flow [23] which was selected for this purpose chiefly on the basis of the reasonable degree of detail to which the appropriate data have been published.

In this paper, we shall be concerned almost exclusively with the turbulent heat transport. The appropriate form of the diffusivity concept can then be written as

$$-\overline{u_i \theta} = D_{ij} (\partial T / \partial x_j)$$

where D_{ij} is the second-order diffusivity tensor. (The diffusivity tensor is not diagonal, or even symmetric; using a combination of experiment in homogeneous shear flows, theory and informed speculation, *Tavoularis* and *Corrsin* [24] have evaluated several components of D_{ij} .) In the simplest case with the dominant mean temperature gradient essentially in the direction x_2 , the GTM gives

$$-\overline{u_2 \theta} = D_{22} (\partial T / \partial x_2) \equiv D (\partial T / \partial x_2) \quad , \quad (1)$$

where D is the diffusivity. It is in this simple form that the GTM will concern us here.

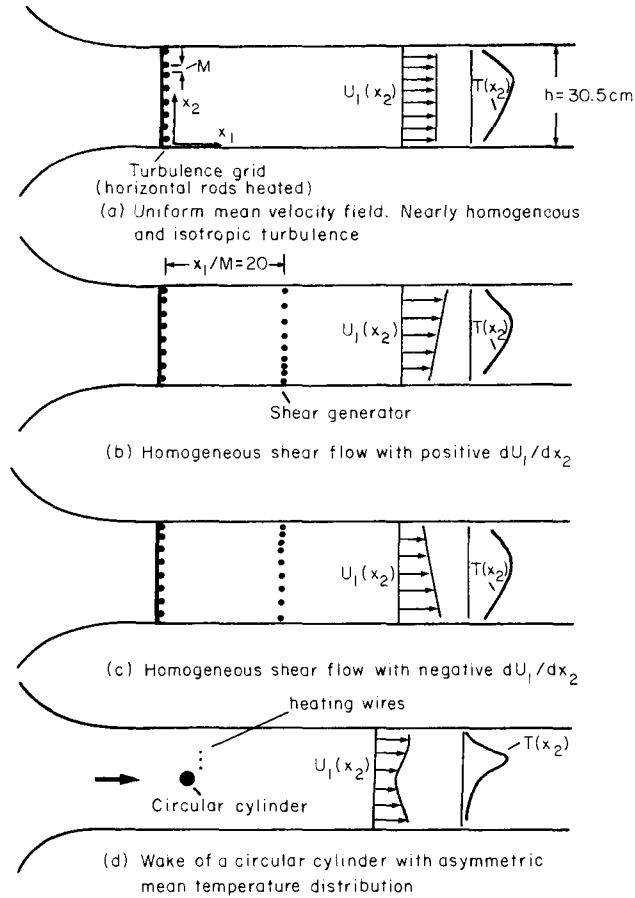
Flow Configuration

Figure 1 shows a schematic representation of the experimental configurations used here. The wind tunnel was of the open-return type with a nominal test section 30 cm × 30 cm, and about 3.65 m long. Air flow was created by two axial fans in tandem. An essentially constant pressure field was created by adjusting the vertical walls.

Three homogeneous flows and one inhomogeneous shear flow were studied. One of the homogeneous flows was the uniform flow produced behind a square-mesh biplane cylindrical-rod grid with 2.54 cm mesh and solidity 0.36. The mean velocity was nominally uniform across the test section. The temperature field was created by electrical heating each of the horizontal rods of the grid separately, so that a desired inhomogeneous mean temperature field could be created (Fig. 1a).

The two other homogeneous flows with nominally uniform positive or negative mean velocity gradient were created by placing a shear generator 20 mesh sizes downstream of the turbulence-generating grid (see Fig. 1b,c). The shear generator is an array of horizontal non-uniformly spaced cylindrical rods [25] and could be inserted in the wind-tunnel such that dU_1/dx_2 could be positive (Fig. 1b) or negative (Fig. 1c). The temperature field was created exactly as in the uniform flow case.

Lastly, the inhomogeneous free shear flow studied here is the wake of a circular cylinder ($d = 1.1$ cm) in which the temperature field was produced by heating three thin parallel wires (diameter 0.127 mm) mounted asymmetrically with respect to the cylinder on a wooden frame which could be inserted (see Fig. 1d) at any of the three locations ($x_1/d = 1.2, 2.3, \text{ and } 4.6$) downstream of the cylinder. Also, the spacing be-



tween the wires, their transverse location with respect to the cylinder and the heating current in each of the wires could be adjusted independently to obtain within limits any desired mean temperature distribution.

Instrumentation

Mean velocity U_{10} along the tunnel centreline was measured with a pitot-static tube. The mean velocity profile $U_1(x_2)$ and the velocity fluctuations u_1 and u_2 were measured with a DISA 55P51 gold-plated X-wire probe, with sensing elements $5 \mu\text{m}$ in diameter and 1 mm in length, powered by two DISA 55D01 constant temperature anemometers; dc power supplies were used to minimize the noise level. The mean temperature profile $T(x_2)$ and the reference temperature upstream of the grid were measured with two Fenwal Electronics GC32M21 thermistor probes. The temperature fluctuation θ was measured with a DISA 55P31 platinum wire probe with the wire length of 0.4 mm and diameter $1 \mu\text{m}$. The temperature wire was positioned vertically at a distance of about 0.5 mm from the nearest wire of the X-wire probe, and was operated at a constant current of 0.3 mA on a home-made constant current source [26]. The operating current was low enough to render the velocity sensitivity of the temperature wire negligible. The temperature contamination of the velocity signals was eliminated by correcting

them with the instantaneous local temperature measured with the temperature wire [27]. The vertical position of the probes was adjusted with a variable speed motor and a gear mechanism.

All signals were amplified and low-pass filtered at an upper cut-off frequency of 5 kHz. The signals were also corrected for noise assuming that the noise is statistically independent of the signal. The signals were digitized and processed on a DEC PDP 11/40 digital computer.

Results in Homogeneous Flows

Mean Velocity and Mean Temperature Distributions

Measurements were made at $x_1/M = 60$ and 128 but, in most cases, only those made at $x_1/M = 60$ are reported here. In all the cases, there was a significant region of two-dimensionality in the mean quantities.

Figure 2 shows the distribution of mean velocity and mean temperature rise for the three homogeneous flows. For the uniform flow experiment, the mean velocity was uniform across the test section to within about 2% of the centreline velocity of 17.2 m s^{-1} . The grid mesh Reynolds number was about 29,100. The two other flows had roughly linearly varying mean velocity profiles (except for the last point in each case on the low velocity side). The centreline velocity U_{10} in both cases was 16.0 m s^{-1} , and $|dU_1/dx_2|$ was 17.9 s^{-1} .

In all three cases, the mean temperature distributions were quite similar. The maximum mean temperature rise of about 2.7°C was low enough to consider heat as a passive scalar. This was also verified by noting that the measured root-mean-square velocity intensities with and without heating were essentially the same. A measure of the inhomogeneity of the temperature field is given by the parameter $(dT/dx_2) L_g/T_{\text{max}}$. In the present experiments, the highest value assumed by this parameter was about 0.5, signifying a sizeable inhomogeneity.

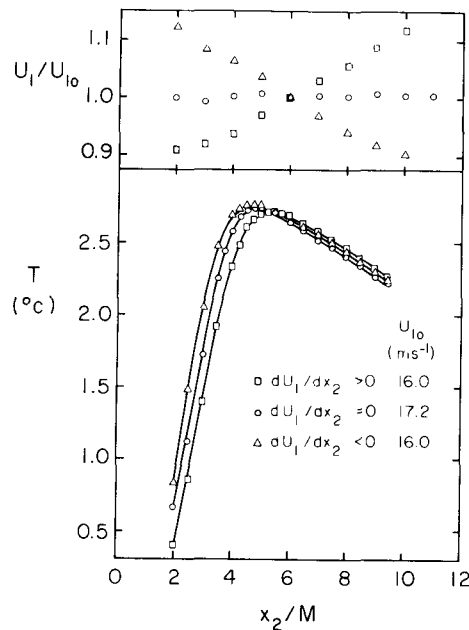


Fig. 2. Transverse distributions of mean velocity and mean temperature

Root-Mean-Square Intensities

Figure 3 shows the transverse distribution of the normalized root-mean-square velocity fluctuations in the central two-thirds of the tunnel height. For the uniform grid flow, both u'_1 and u'_2 are uniform to within $\pm 5\%$. The ratio $u'_1/u'_2 \cong 1.15$, quite comparable to that in other similar flows [28]. For the shear flows, on the other hand, there is a $\pm 12\%$ variation in u'_1/U_{10} and about $\pm 8\%$ variation in u'_2/U_{10} . For the present purposes, these distributions were considered sufficiently homogeneous in the transverse direction. On the average, $u'_1/u'_2 = 1.23$. At $x_1/M = 128$, the turbulence intensity distributions are homogeneous to a somewhat better accuracy. Figure 4 shows the transverse distribution of the normalized root-mean-square temperature fluctuation.

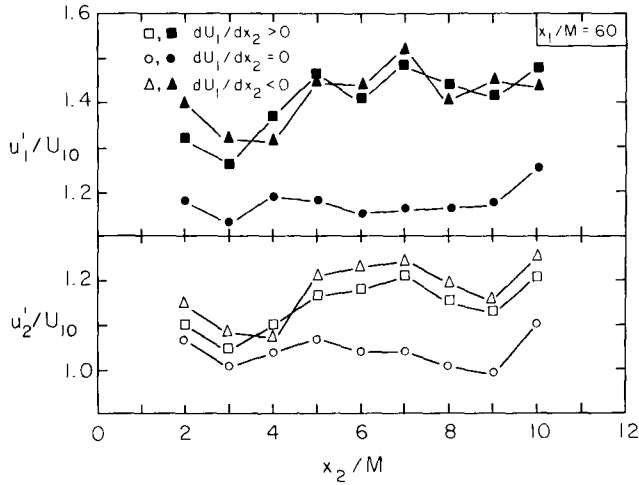


Fig. 3. Transverse variation of turbulence intensities

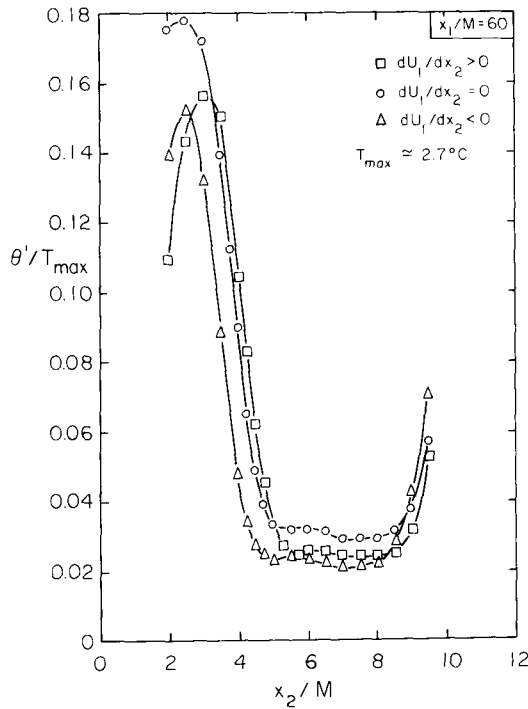


Fig. 4. Transverse distribution of the root-mean-square temperature fluctuation

Heat Transport in the x_2 -Direction

Figure 5 shows how at $x_1/M = 60$ the correlation coefficient $-\overline{u_2\theta}/u_2'\theta'$ varies with respect to x_2/M . It is seen in comparison with Fig. 2 that $\overline{u_2\theta}$ changes sign essentially where the mean temperature gradient vanishes. Figure 6 in which $\overline{u_2\theta}$ is plotted against the corresponding total values of dT/dx_2 shows this more clearly.

Data are presented for both $x_1/M = 60$ and 128. A 6th order polynomial was fitted to the measured mean temperature distribution to obtain dT/dx_2 . The estimated error bounds for both quantities are shown in the figure. It is clear that in all three cases $\overline{u_2\theta}$ is zero when dT/dx_2 is zero, and a gradient transport model with constant diffusivity is quite satisfactory.

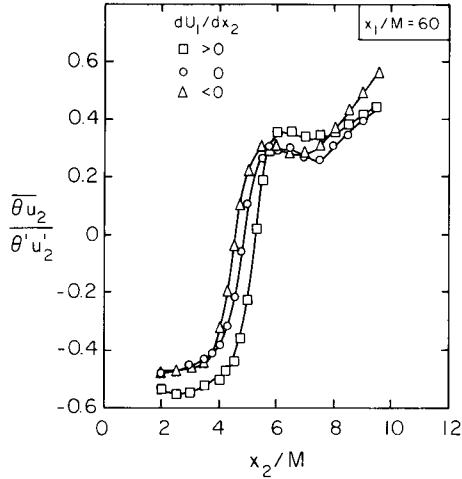


Fig. 5. The coefficient of correlation between transverse velocity and temperature fluctuations

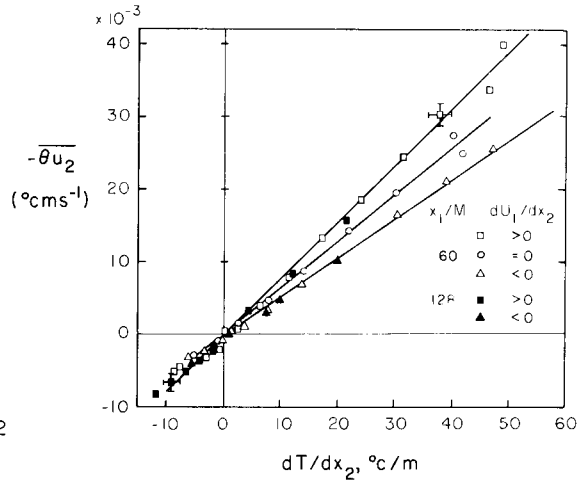


Fig. 6. The variation of the turbulent heat flux with mean temperature fluctuations

Table 1. The turbulent diffusivity, and the characteristic length and time scales of turbulent diffusion in the present homogeneous flows

dU_1/dx_2	D/γ	l [cm]	τ [ms]	l/L_g
> 0	36.6	0.42	22.8	0.11
= 0	30.5	0.36	20.1	0.35
< 0	25.5	0.29	15.8	---

Table 2. The turbulent diffusivity, and the characteristic length and time scales of turbulent diffusion in the *Tavoularis-Corrsin* flow [27]

x_1/h	D/γ	l [cm]	τ [ms]	l/L_g
6	59.5	0.44	15.4	0.11
7.5	72.5	0.48	15.2	0.11
9.5	93.0	0.53	14.6	0.10
11.0	114.0	0.59	14.5	0.10

The diffusivities evaluated from slopes of the straight lines in Fig. 6 are given in Table 1 (the molecular diffusivity $\gamma = 0.21 \times 10^{-4} \text{ m}^2 \text{ s}^{-1}$). Interestingly, the turbulent transport in the case with $dU_1/dx_2 > 0$ is more efficient, and that in the case with $dU_1/dx_2 < 0$ is less efficient, than that in the uniform velocity flow. The reason for this is not immediately apparent (for example, from the equation for $\overline{u_2\theta}$, since the mean velocity gradient does not appear explicitly in such an equation).

For the case of constant diffusivity, we can write [29]

$$D = Vl = V^2 \tau \quad . \quad (2)$$

Presumably, V and τ must respectively be the root-mean-square velocity and integral time scale of velocity following a material point. However, we shall assume that $V = u'_2$ (this is strictly true only for stationary homogeneous turbulence), and compute the values of l and τ from the measured diffusivity. These are also shown in Table 1.

In the present flow with $dU_1/dx_2 > 0$, the measured (Eulerian) transverse integral scale of turbulence L_g at $x_1/M = 70$ was about 40 mm. (The integral length scales here and elsewhere in this paper were obtained by evaluating the area up to the first crossing under the appropriate correlation curve. For a discussion of this point, see [30]). It should be remarked that the integral length scale in this flow is one order of magnitude larger than the length scale l characteristic of turbulent diffusion. No measurements of L_g were made for the flow with $dU_1/dx_2 < 0$, but the same conclusion can be expected to hold here also. The implication is that for homogeneous uniformly sheared flows, the eddies most effective in turbulent transport are *not* of the order of the integral scale, but an order of magnitude smaller. On the other hand, for the homogeneous non-sheared turbulence ($dU_1/dx_2 = 0$), L_g estimated from the relation [31]

$$L_g/M = 0.065 (x_1/M - 3)^{0.4}$$

is about 8.3 mm, which is only about $2^{1/2}$ times as large as l .

Asymmetrically Heated Wake

Measurements were made for several configurations of the heating wires and the wake generator, but results are presented here only for that shown in Fig. 7. Measurements were made only at one station ($x_1/d \cong 100$). It would have been desirable to have made the measurements further downstream (where the flow would be self-preserving to a better degree of approximation), but the limitations of accuracy in heat transport measurements for small T led to this choice. Figure 7 shows transverse profiles of normalized velocity defect w/w_0 ($w_0 = 1.78 \text{ m s}^{-1}$), u'_2/w_0 , T , θ'/T_{max} and L_f/d ; here L_f was obtained by evaluating the area up to the first crossing under the auto-correlation function of u_1 and converting the resulting integral time scale to a length scale via Taylor's "frozen field" approximation. It is seen that even at $x_1/d \cong 100$, the presence of the wires in the wake results in a slight asymmetry in the velocity near the maximum defect region, and stronger asymmetries in u'_2 and L_f profiles.

Figure 8a shows a plot of the heat flux $-\overline{u_2\theta}$ and the mean temperature gradient $\partial T/\partial x_2$ at several points across the wake. Clearly, there is a small but finite region (the shaded region in the figure) in which the heat flux and the mean temperature gradient are of opposite sign implying negative diffusivity, or heat transport against the mean temperature gradient.

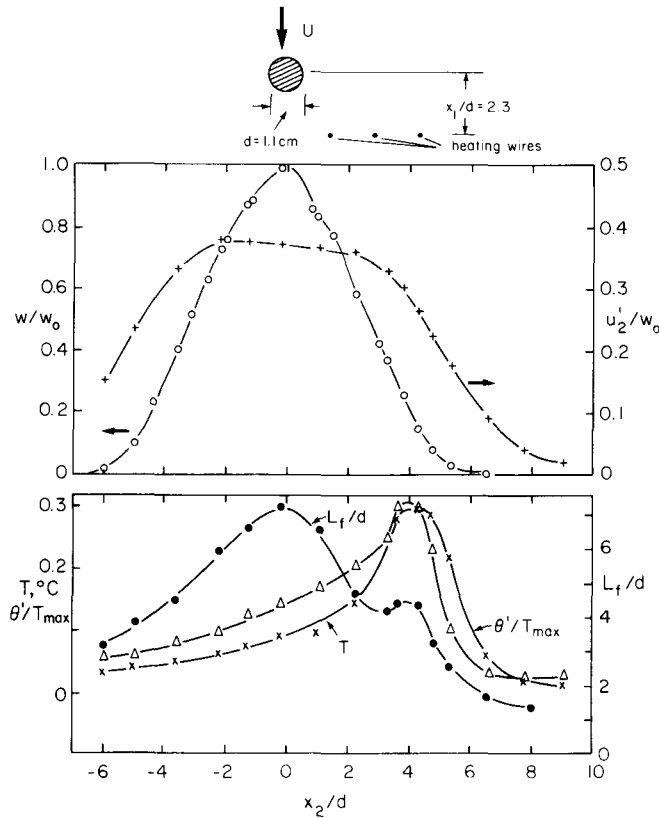


Fig. 7. A representative experimental configuration of the circular cylinder/heating-wire combination, and the resulting transverse distributions of mean defect velocity and temperature rise

A more direct demonstration of the inadequacy of the GTMs is given in Fig. 8b which shows that $-\overline{u_2\theta}$ when plotted against $\partial T/\partial x_2$ forms a closed loop. (If a GTM were applicable, the loop would collapse on to a single curve through the origin; if the diffusivity were also constant, the curve would be a straight line.) For the discussion to follow, the rough correspondence between the various key points of this loop and their physical location is indicated by the use of the same letters A, B, C, D and E in Fig. 8a, b, and the inset to Fig. 8b. Large negative x_2/d (say, around A in the inset) correspond to the vicinity of the origin in Fig. 8b. As x_2/d increases (algebraically), both $\partial T/\partial x_2$ and $-\overline{u_2\theta}$ increase until at B the (positive) maximum value of $\partial T/\partial x_2$ is reached. Beyond B, $\partial T/\partial x_2$ decreases but $-\overline{u_2\theta}$ does not keep pace with $\partial T/\partial x_2$ and is finite and large even in the vicinity of C where $\partial T/\partial x_2$ is small. For even larger x_2/d , $\partial T/\partial x_2$ is negative (path CD) until the negative maximum of the temperature gradient is attained at D; around D, $-\overline{u_2\theta}$ is still decreasing (see Fig. 8a), however. The path DE constitutes the return to $\partial T/\partial x_2 = 0$ as x_2/d approaches large positive values.

Corresponding regions in which the turbulent momentum transport $-\overline{u_1u_2}$ occurs against the direction of mean velocity gradient have been observed in many different flow situations [10–20]. These regions have been called regions of “energy reversal” [13] or, more commonly in the later literature, as regions of “negative production”, although the appropriateness of either term has been questioned. For example, it has been pointed out [32] that the total production terms are given by $-\overline{u_iu_j} \partial U_i/\partial x_j$, and that in the regions where $-\overline{u_1u_2} (\partial U_1/\partial x_1)$ is negative, the other production terms $-(u_1^2 - u_2^2) \partial U_1/\partial x_1 - \overline{u_1u_2} \partial U_2/\partial x_1$ are positive and (though small) of the right

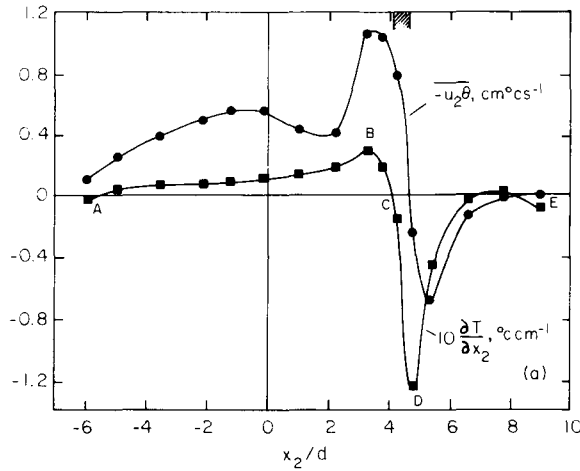
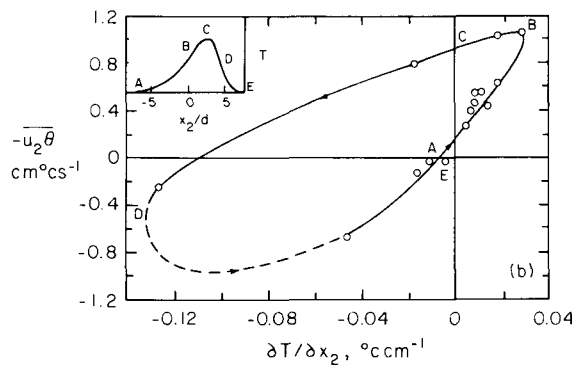


Fig. 8 a,b. The variation of turbulent heat flux (a) across the flow width and (b) with mean temperature gradient for the asymmetrically heated flow



magnitude to counteract locally the negative values of $-\overline{u_1 u_2} \partial U_1 / \partial x_2$. However, this conclusion is negated by other measurements [14, 33] in which all the production terms except $-\overline{u_1 u_2} (\partial U_2 / \partial x_1)$ were measured. (However, in these two latter cases, the magnitude of the negative values of the total production is very small.) Lastly, we mention *Hinze's* [20] conclusion that even if the sum-total of production terms is negative, it does not imply energy transfer back to the mean flow.

In the heat transfer case, there are fewer measurements of the θ^2 -production terms [18, 23, 34], but the balance of evidence does suggest that the total thermal production terms

$$-\overline{u_2 \theta} \partial T / \partial x_2 + \overline{u_1 \theta} \partial T / \partial x_1$$

add up to negative values in some small flow region. In the present wake, mean temperature profiles were not measured sufficiently closely to evaluate $\partial T / \partial x_1$ accurately, but rough estimates suggest that the inclusion of $-\overline{u_1 \theta} (\partial T / \partial x_1)$ does not alter the sign of total production in any substantial way.

'Generalizations' of GTM

One obvious way to generalize the GTM for inhomogeneous situations is to replace the constant diffusivity by a space-dependent diffusivity. *Corrsin* [8] has noted that this is not a self-consistent generalization to adopt. Using a heuristic analogy based on gen-

eralized one-dimensional random walks, he inferred an alternative expression for the mean flux \bar{F} of a passive scalar contaminant (concentration Γ) with a dominant mean concentration gradient ($\partial\Gamma/\partial x_2$). *Corrsin's* analysis is based essentially on a Taylor expansion for inhomogeneities and unsteadiness in the transport, with (effectively) the characteristic length scale l as the small parameter. His analysis shows that to $O(l^2)$ in steady transport

$$-\bar{F} = D (\partial\Gamma/\partial x_2) + l\Gamma (\partial V/\partial x_2) . \quad (3)$$

The expression is valid for unsteady transport also, but to $O(l)$.

Another generalization of simple GTM has been proposed by *Lumley* [21], based on the power series expansion of a continuous probability density function for displacement of tagged particles. The formulation appears to be in much the same spirit as a ‘‘Kramers-Moyal expansion’’. Keeping only the first two terms of this infinite series, *Lumley* showed that the net integrated flux is given by:

$$\bar{F} = \bar{\Gamma} \frac{d(\overline{\Delta x_2})}{dt} - \frac{1}{2} \frac{\partial}{\partial x_2} \left[\Gamma(x_2) \frac{d(\overline{\Delta x_2})^2}{dt} \right] . \quad (4)$$

Lumley argued that for an almost homogeneous situation

$$\frac{d(\overline{\Delta x_2})}{dt} = \frac{1}{4} \frac{\partial}{\partial x_2} \frac{d(\overline{\Delta x_2})^2}{dt}$$

so that Eq. (4) becomes

$$-\bar{F} = D \frac{\partial \bar{\Gamma}}{\partial x_2} + \frac{1}{2} \bar{\Gamma} \frac{\partial D}{\partial y} , \quad (5)$$

where we have used the simple result from the Brownian motion theory that the diffusivity D is given by

$$D = \frac{1}{2} \frac{d(\overline{\Delta x_2})^2}{dt} .$$

For a homogeneous situation, $d(\overline{\Delta x_2})/dt = 0$, so that Eq. (4) reduces to the classical GTM.

Kranenburg [22] derived an alternative expression based on the Lagrangian formulation of particle dispersion. If one neglects viscosity, the concentration of a passive scalar quantity is conserved along a fluid particle trajectory, and one can then write:

$$\Gamma(\mathbf{x}, t) - \Gamma\left(\mathbf{x} - \int_{t-\tau_K}^t V(t'|\mathbf{x}, t) dt', t - \tau_K\right) = 0$$

where $V(t'|\mathbf{x}, t)$ is the time (t') dependent Lagrangian velocity of the fluid particle passing through \mathbf{x} at time t . *Kranenburg* applied the mean value theorem to the integral in the above equation, and took the analysis through the following steps. First, he assumed that τ_K was *small* enough to permit the particle trajectories to be approximated by straight lines (with the stochasticity entering into the problem through the stochasticity in τ_K). Then, using the Eulerian conservation equation for the scalar function Γ evaluated in the preceding steps, he obtained, in the limit of *large* diffusion times, the result that

$$-\bar{F} = D (\partial\Gamma/\partial x_2) + l \frac{\partial}{\partial x_2} (D\partial\Gamma/\partial x_2) \quad . \quad (6)$$

The self-consistency of the assumptions is not immediately obvious.

All these three models share a few things in common. They introduce no additional adjustable constants into the respective expressions and seek to obtain (in a more or less rational framework) corrections necessitated by inhomogenities in a process that is basically gradient-transport type; in some sense, the departures from the GTM are perceived to be small.

There is general awareness that in turbulent shear flows, transport occurs not only by the diffusive motion of the small eddies (as envisaged in the GTMs) but also by the motion of large eddies comparable in size to the flow width. It appears unlikely that the transport due to these bulk motions will be proportional to the local concentration gradient; if the large-scale motion is potent in its transport characteristics, it appears equally unlikely that the total transport can be successfully evaluated by applying small corrections to the gradient transport type mechanism. Motivated by these considerations, *Townsend* [35] made a rough model for the total transport. In its simplest sense, the model can be represented by

$$-\bar{F} = D (\partial\Gamma/\partial x_2) + V_c \Gamma_{\max} \quad (7)$$

where V_c is a bulk convection velocity (to be determined externally) and Γ_{\max} is the maximum concentration difference within the flow field.

Motivated essentially by these considerations, *Beguier et al.* [23] proposed a somewhat more specific model for the bulk convection. Their model is no more than a straightforward analogy to *Beguier's* [36] momentum transport model, whose brief description is therefore approximate. Let A and B be the two points in the flow where $\partial U_1/\partial x_2 = 0$ and $\bar{u}_1 \bar{u}_2 = 0$, respectively, and l_m be the distance between A and B. Region AB is the negative production region. Since this region is generally thin, the mean concentration gradient at B can be written as

$$\left(\frac{\partial U_1}{\partial x_2}\right)_B = l_m \left(\frac{\partial^2 U_1}{\partial x_2^2}\right)_A \quad .$$

Beguier then models the momentum transport due to bulk motion by

$$D_m \left(\frac{\partial U_1}{\partial x_2}\right)_B = D_m l_m \left(\frac{\partial^2 U_1}{\partial x_2^2}\right)_A \quad ,$$

where D_m is the momentum eddy diffusivity which itself is assumed to be given by

$$D_m = K_m W^2 \left(\frac{\partial q'}{\partial x_2}\right)_A$$

with W as the 'width' of the flow and K_m as a free constant. In analogy to this model, the total heat transport can be written as

$$-\bar{u}_2 \bar{\theta} = D (\partial T/\partial x_2) + K_\theta l_\theta^3 (\partial q'/\partial x_2) (\partial^2 T/\partial x_2^2) \quad (8)$$

where K_θ is a constant and $(\partial^2 T/\partial x_2^2)$ is to be evaluated at the point where $(\partial T/\partial x_2) = 0$. This is effectively the model given in [23].

Test of Generalized Models

All expressions for the models briefly discussed above are given to the first order of 'correction'. A knowledge of the Lagrangian root-mean-square velocity and integral time scales across the shear flows under consideration is now needed, but is at the moment not available. For the specific purposes of testing these models, we shall replace l by the Eulerian integral scale L_f , V by the Eulerian root-mean-square velocity u'_2 and the diffusivity D by $L_f u'_2$. A more appropriate definition based on Lagrangian scales would presumably differ from the present one, but would not lead to qualitatively different conclusions. Particularizing the various models to heat transport (i.e., replacing the concentration Γ by the temperature T), we have:

$$-\overline{u_2 \theta} = D (\partial T / \partial x_2) \equiv R_G \quad (9a)$$

$$-\overline{u_2 \theta} = D (\partial T / \partial x_2) + L_f T (\partial u'_2 / \partial x_2) \equiv R_C \quad (9b)$$

$$-\overline{u_2 \theta} = D (\partial T / \partial x_2) + (T/2) (\partial D / \partial x_2) \equiv R_L \quad (9c)$$

$$-\overline{u_2 \theta} = D (\partial T / \partial x_2) + L_f \partial / \partial x_2 (D \partial T / \partial x_2) \equiv R_K \quad (9d)$$

$$-\overline{u_2 \theta} = D (\partial T / \partial x_2) + K_\theta l_\theta^3 (\partial q' / \partial x_2) (\partial^2 T / \partial x_2^2) \equiv R_B \quad (9e)$$

$$-\overline{u_2 \theta} = D (\partial T / \partial x_2) + V_c T_{\max} \equiv R_T \quad (9f)$$

Referring now to Fig. 8b, any improved alternative to the GTM must be capable of collapsing the closed loop on to a single curve or nearly so. This is the simple criterion

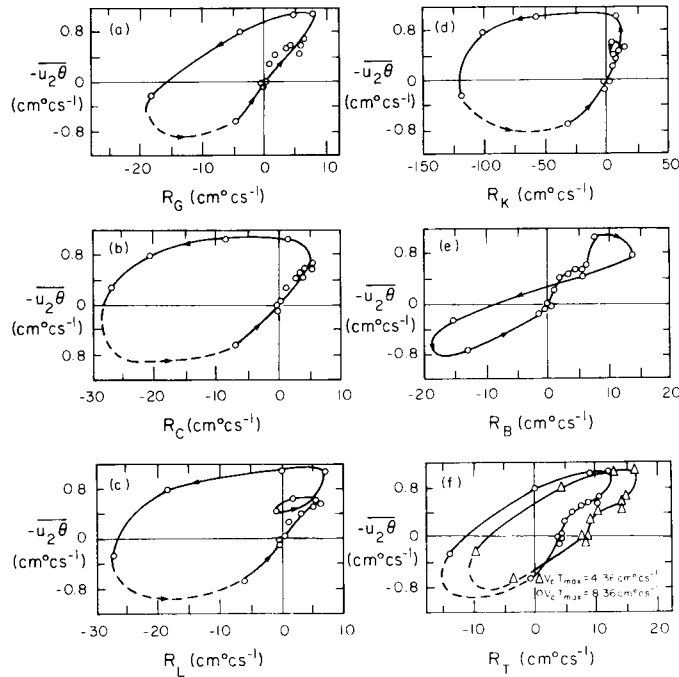


Fig. 9. A test of generalizations of GTM for the present asymmetrically heated flow

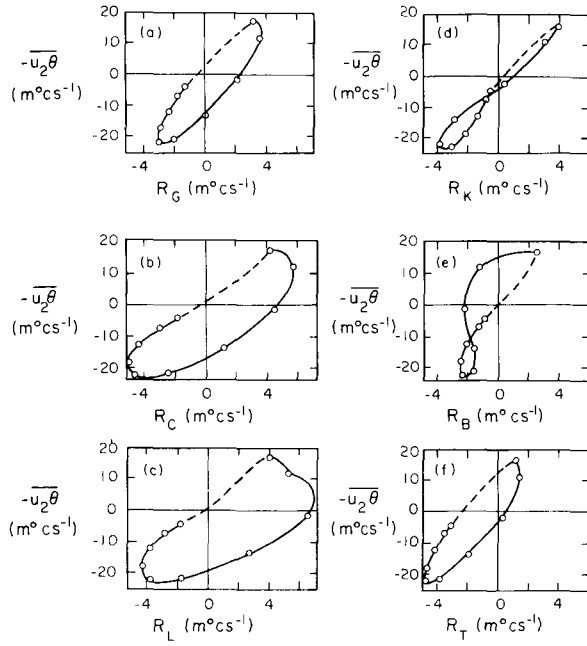


Fig. 10. A test of generalizations of GTM for asymmetrically heated mixing layer [23]

that we shall adopt as a measure of success of any given model. From both Figs. 9 and 10, the models due to *Corrsin* [8] and *Lumley* [21] appear to aggravate rather than improve the situation. The *Kranenburg* model appears to work reasonably well for the mixing layer data [23], but has poor performance in the present flow. For testing Eq. (9e) using the present flow data, we have replaced q' by $[3(u_1^2 + u_2^2)/2]$. This and other assumptions implied in Eq. (8) introduce an uncertainty in the precise value of K_θ . We tried several values of K_θ , and the best value (Fig. 9e) was found to be 0.015. Note that in contrast to the suggestion of [23], this constant assumed a positive value: the significance of a model whose constant changes sign from one flow to another is not clear. In the simple version of *Townsend's* model, the correction due to the bulk transport is a constant number on the right-hand side, and this can only translate the closed loop without either shrinking or enlarging it. The effect is shown in Figure 9f for two values of the correction, and in Figure 10f for one.

Discussion

In the homogeneous shear flows examined here, the length scale characteristic of the eddies most effective in transporting heat were found to be small compared with the integral scale of turbulence (Table 1), or the scale of inhomogeneity of the temperature field. The transport is thus mainly a diffusive effect due to these small eddies and it comes as no surprise that the GTM works as well as it does. This can be shown also formally by noting that all the criteria listed by *Corrsin* [8] as being necessary for the GTM to work are satisfied in these flows. The only one requiring some comment is the condition that

$$\frac{l^2}{24} \frac{(\partial^3 T / \partial x_2^3)}{(\partial T / \partial x_2)} \ll 1 \quad . \quad (10)$$

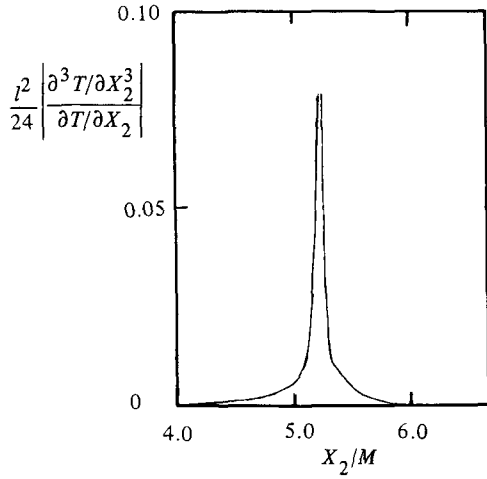


Fig. 11. A test of validity of the GTM for turbulent transport in the homogeneous flow with $dU_1/dx_2 = U$. Note that the required condition (10) is violated in a very localized region, which is thus of no consequence

This is effectively a size limitation on the “mean free path” l of the diffusion process. Clearly, there is always a region in the flow where the above inequality is not satisfied, but this is such a local aberrant (see Fig. 11) that its effects do not manifest significantly.

Our experiments have emphasized that the GTM which appears perfectly adequate with a constant diffusivity for the homogeneous flows cannot handle inhomogeneous flows even qualitatively. The chief difference between the homogeneous and inhomogeneous shear flows is the dominance of the large structures in the latter; it appears that the large structures are responsible for a sizeable fraction of the transport process, and it is in the modelling of these effects that none of the generalizations of the GTM discussed earlier has had reliable success. One of the currently held views is that a turbulent shear flow is essentially a consequence (and not the cause) of these transport-efficient large structures and their mutual interactions. If this view is correct, an altogether different approach, which does not even invoke a mean field, is necessary before the problem can be resolved.

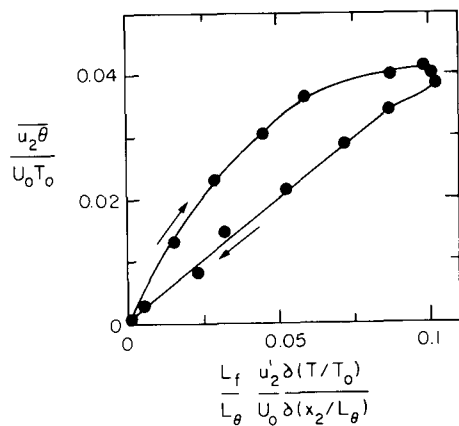


Fig. 12. The variation of turbulent heat flux with mean temperature gradient in a symmetrically heated co-flowing jet [37]

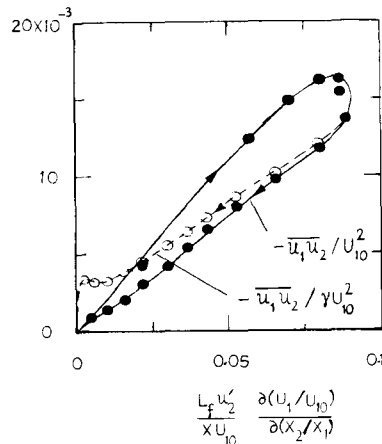


Fig. 13. The variation of turbulent momentum flux with the mean velocity gradient in an axisymmetric jet [38]. Notice how the introduction of the intermittency factor ‘over-corrects’ the heat flux values

Finally, we examine briefly the reason why GTM has often been claimed to work well in some free shear flows. Figure 12 shows a plot of $\overline{u_2\theta}$ vs $(\partial T/\partial x_2)$ – now appropriately normalized – for one half of a symmetrically heated co-flowing jet [37]. It is again seen that the data form a loop instead of a single curve. However, the flow symmetry about the centreline forces both $\overline{u_2\theta}$ and $\partial T/\partial x_2$ to be zero at the same point, so that the return part of the loop is now constrained to go through the origin. This results in a much smaller loop than would be the case if asymmetries existed. This is the reason for the apparent success of the GTM in symmetric flows; the large eddies are no less effective in transporting heat in these flows.

So far, we have concentrated on the heat transport, but the present conclusions should be relevant also for the momentum transport. We may now briefly consider the momentum transport in an axisymmetric jet [38], and examine the applicability of the GTM in the context of the smallness or otherwise of the appropriate loop. Figure 13 shows that a plot of $\overline{u_1 u_2}$ as a function of $\partial U_1/\partial x_2$ indeed forms a loop that is not too wide, again for reasons of imposed boundary conditions; GTM should thus work reasonably, as indeed it does. If one took account of the outer intermittency of the jet, it is seen from Fig. 13 that no qualitative changes in the conclusions result. Towards the outer edge, the intermittency ‘over-corrects’ the expectation from the GTM.

Acknowledgement. This research was supported by the Atmospheric Science Division of the National Science Foundation.

References

1. Monin, A.S., Yaglom, A.M.: *Statistical Fluid Mechanics: Mechanics of Turbulence*, ed. by J.L. Lumley. Vol. 1 M.I.T. Press, Cambridge (1971)
2. Hinze, J.O.: *Turbulence* 2nd ed. McGraw-Hill, New York (1976)
3. Launder, B.E.: “Heat and Mass Transport”, in *Turbulence*, ed. by P. Bradshaw, Topics in Applied Physics, Vol. 12 Springer, Berlin, Heidelberg, New York 1978 pp. 231–287
4. Cohen, D.S., Murray, J.D.: A generalized diffusion model for growth and dispersal in a population. *J. Math. Biol.* 12, 237–249 (1981)
5. Saltzman, B.: A survey of statistical dynamical models in the terrestrial climate. *Adv. Geophys.* 20, 183–304 (1978)
6. Batchelor, G.K.: Note on free turbulent flows, with special reference to the two-dimensional wake. *J. Aeronaut. Sci.* 17, 441–445 (1950)
7. Corrsin, S.: Heat transfer in isotropic turbulence. *J. Appl. Phys.* 23, 113–118 (1952)
8. Corrsin, S.: Limitations of gradient transport models in random walks and in turbulence. *Adv. Geophys.* 18A, 25–60 (1974)
9. Saffman, P.G.: “Problems and Progress in the Theory of Turbulence”, in *Structure and Mechanism of Turbulence II*, ed. by H. Fiedler, Lecture Notes in Physics, Vol. 7 (Springer, Berlin, Heidelberg, New York 1978), pp. 183–304
10. Eskinazi, S., Yeh, H.: An investigation of fully developed turbulent flows in a curved channel. *J. Aeronaut. Sci.* 23, 23–31 (1956)
11. Mathieu, J., Tailland, A.: Etude d’un jet plan dirigé tangentiellement à une paroi. *C.R. Acad. Sci.* 256, 2768–2771 (1963)
12. Gee, M.T., Bradshaw, P.: Turbulent wall jets with and without external stream. *NPL Bull.* 3252 (1960)
13. Eskinazi, S., Erian, E.F.: Energy reversal in turbulent flows. *Phys. Fluids* 12, 1988–1998 (1969)
14. Erian, E.F.: Influence of pressure gradient on turbulent flow with asymmetric mean velocity. *ASME-J. Appl. Mech.* 91, 901–904 (1969)
15. Hanjalic, K., Launder, B.E.: Fully developed asymmetric flow in a plane channel. *J. Fluid Mech.* 51, 301–335 (1972)
16. Palmer, M.D., Keffer, J.F.: An experimental investigation of an asymmetrical turbulent wake. *J. Fluid Mech.* 53, 593–610 (1972)
17. Fabris, G.: “Conditionally Sampled Turbulent Thermal and Velocity Fields in the Wake of a Warm Cylinder and Its Interaction with an Equal Cool Wake”; Ph.D. dissertation, Illinois Institute of Technology (1979)

18. Charney, G., Schon, J.P., Alcaraz, E., Mathieu, J.: "Thermal Characteristics of a Turbulent Boundary Layer with Inversion of Wall Heat Flux", Proc. of the Symposium on Turbulent Shear Flows, Penn. State University, University Park, 1977, pp. 15, 47–15.55
19. Morel, R., Awad, M., Schon, J.P., Mathieu, J.: "Experimental Study of an Asymmetric Thermal Wake", in *Structure and Mechanism of Turbulence I*, ed. by H. Fiedler. Lecture Notes in Physics, Vol. 75 (Springer, Berlin, Heidelberg, New York, 1978) pp. 36–45
20. Hinze, J.O.: Turbulent flow regions with shear stress and mean velocity gradient of opposite sign. Appl. Sci. Res. 22, 168–175 (1970)
21. Lumley, J.L.: Modelling turbulent flux of passive scalar quantities in inhomogeneous flows. Phys. Fluids 18, 619–621 (1975)
22. Kranenburg, C.: On the extension of gradient-type transport to turbulent diffusion in inhomogeneous flows. Appl. Sci. Res. 33, 163–175 (1977)
23. Beguier, C., Fulachier, L., Keffer, J.F.: The turbulent mixing layer with an asymmetrical distribution of temperature. J. Fluid Mech. 89, 561–587 (1978)
24. Tavoularis, S., Corrsin, S.: "Theoretical and Experimental Determination of the Turbulent Diffusivity Tensor in Homogeneous Turbulent Shear Flow", Proc. of the 3rd Symposium on Turbulent Shear Flows, University of California, Davis, 1981, pp. 15.24–15.27
25. Rose, W.G.: Results of an attempt to generate a homogeneous turbulent shear flow. J. Fluid Mech. 25, 97–120 (1966)
26. Tavoularis, S.: A Circuit for the measurement of instantaneous temperature in heated turbulent flows. J. Phys. E 11, 21–23 (1978)
27. Tavoularis, S., Corrsin, S.: Experiments in nearly homogeneous turbulent shear flow with a uniform mean temperature gradient. Part 1, J. Fluid Mech. 104, 311–347 (1981)
28. Comte-Bellot, G., Corrsin, S.: The use of a contraction to improve the isotropy of grid-generated turbulence. J. Fluid Mech. 25, 657–682 (1966)
29. Corrsin, S.: "Some Current Problems in Turbulent Shear Flow", in *Naval Hydrodynamics*, Proc. of the 1st Symp. on Naval Hydrodynamics, ed. by F. Sherman Publication No. 515, (National Academy of Science, National Research Council, Washington, D.C. 1957) pp. 373–400
30. Comte-Bellot, G., Corrsin, S.: Simple Eulerian time correlation of full and narrow-band velocity signals in grid-generated, isotropic turbulence. J. Fluid Mech. 48, 273–337 (1971)
31. Sreenivasan, K.R., Tavoularis, S., Henry, R., Corrsin, S.: Turbulent fluctuations and scales in grid-generated turbulence. J. Fluid Mech. 100, 597–621 (1980)
32. Wilson, J.D.: Turbulent transport of mean kinetic energy in countergradient shear stress regions. Phys. Fluids 17, 674–675 (1974)
33. Beguier, C.: Mesures de tensions de Reynolds dans un écoulement dissymétrique en régime turbulent incompressible. J. Méc. 4, 319–334 (1965)
34. Fulachier, L., Keffer, J.F., Beguier, C.: Production negative de fluctuations turbulentes de température dans le case d'un créneau de chaleur s'épanouissant dans une zone de mélange", C.R. Acad. Sci. 280, pp. 519–522 (1975)
35. Townsend, A.A.: *The Structure of Turbulent Shear Flows*, (University Press, Cambridge 1956)
36. Beguier, C.: Ecoulements plans dissymétriques en régime turbulent incompressible, par. C.R. Acad. Sci. A268, 69–72 (1969)
37. Antonia, R.A., Prabhu, A. Stephenson, S.E.: Conditionally sampled measurements in a heated turbulent jet. J. Fluid Mech. 72, 455–580 (1975)
38. Wagnanski, I.J., Fiedler, H.E.: Some measurements in the self-preserving jet. J. Fluid Mech. 38, 577–612 (1969)